

One-Dimensional Variational Retrieval Algorithm of Temperature, Water Vapor, and Cloud Water Profiles From Advanced Microwave Sounding Unit (AMSU)

Quanhua Liu and Fuzhong Weng

Abstract—The measurements from satellite microwave imaging and sounding channels are simultaneously utilized through a one-dimensional (1-D) variation method (1D-var) to retrieve the profiles of atmospheric temperature, water vapor and cloud water. Since the radiative transfer model in this 1D-var procedure includes scattering and emission from the earth's atmosphere, the retrieval can perform well under all weather conditions. The iterative procedure is optimized to minimize computational demands and to achieve better accuracy. At first, the profiles of temperature, water vapor, and cloud liquid water are derived using only the AMSU-A measurements at frequencies less than 60 GHz. The second step is to retrieve rain and ice water using the AMSU-B measurements at 89 and 150 GHz. Finally, all AMSU-A/B sounding channels at 50–60 and 183 GHz are utilized to further refine the profiles of temperature and water vapor while the profiles of cloud, rain, and ice water contents are constrained to those previously derived. It is shown that the radiative transfer model including multiple scattering from clouds and precipitation can significantly improve the accuracy for retrieving temperature, moisture and cloud water. In hurricane conditions, an emission-based radiative transfer model tends to produce unrealistic temperature anomalies throughout the atmosphere. With a scattering-based radiative transfer model, the derived temperature profiles agree well with those observed from aircraft dropsondes.

Index Terms—Advance Microwave Sounding Unit (AMSU), one-dimensional variation (1D-var).

I. INTRODUCTION

THE Advance Microwave Sounding Unit (AMSU) measurements are increasingly utilized to derive a variety of atmospheric and surface parameters such as total precipitable water, cloud liquid and ice water, as well as surface snow and sea ice concentration [1], [2]. These products are now routinely generated from the AMSU measurements at a few window channel frequencies which are insensitive to the vertical structures of atmospheric profiles [1]. In particular, atmospheric parameters such as vertically integrated water vapor and cloud liquid water can be derived analytically over oceans where the surface emissivity is low and relatively uniform, and the atmospheric emission from clouds and water vapor is predominant [3].

Manuscript received April 30, 2004; revised December 2, 2004. The views expressed in this publication are those of the authors and do not necessarily represent those of the National Oceanic and Atmospheric Administration.

Q. Liu is with the QSS Group, Inc., Camp Springs, MD 20746 USA (e-mail: Quanhua.Liu@noaa.gov).

F. Weng is with the Sensor Physics Branch, National Oceanic and Atmospheric Administration, National Environmental Satellite, Data, and Information Service, Office of Research and Applications, Camp Springs, MD 20746 USA.

Digital Object Identifier 10.1109/TGRS.2004.843211

TABLE I

AMSU INSTRUMENT CHARACTERISTICS. THE CENTER FREQUENCY FOR AMSU CHANNELS 9–14 IS 57.29 GHz. FOR CHARACTERISTICS, REFER TO THE NOAA KLM USER'S GUIDE (<http://www2.ncdc.noaa.gov/docs/klm/>)

Channel Number	Center Frequency (GHz)	Number of Pass Bands	Band width (MHz)	Center frequency stability (MHz)	NEΔT (K)
1	23.80	1	251	10	0.30
2	31.40	1	161	10	0.30
3	50.30	1	161	10	0.40
4	52.80	1	380	5	0.25
5	53.59 ± 0.115	2	168	5	0.25
6	54.40	1	380	5	0.25
7	54.94	1	380	10	0.25
8	55.50	1	310	0.5	0.25
9	57.29 = fo	1	310	0.5	0.25
10	fo ± 0.217	2	76	0.5	0.40
11	fo ± 0.322 ± 0.048	4	34	0.5	0.40
12	fo ± 0.322 ± 0.022	4	15	0.5	0.60
13	fo ± 0.322 ± 0.010	4	8	0.5	0.80
14	fo ± 0.322 ± 0.004	4	3	0.5	1.20
15	89.00	1	2000	50	0.50
16	89.00	1	5000	50	2.00
17	150	1	4000	50	2.00
18	183±1	1	1000	30	2.00
19	183±3	2	2000	30	2.00
20	183±7	2	4000	30	2.00

This study develops a new one-dimensional (1-D) variation (1D-var) system to derive the profiles of atmospheric parameters such as temperature, water vapor, and cloud hydrometeors over land and oceans by using the measurements from AMSU window and sounding channels. An advanced radiative transfer model including scattering, polarization, and surface emissivity models are developed and integrated as part of the 1D-var retrieval system. With the advanced microwave emissivity model [4], the retrieval of total precipitable water and cloud liquid water is extended over land. The scattering radiative transfer model allows for an algorithm applicable under all weather conditions. The combined use of both microwave window and sounding channels makes it possible to simultaneously derive the cloud water profiles in addition to temperature and water vapor profiles. This integrated approach will lead to the fundamental developments of more advanced microwave products from future satellite microwave instruments that carry onboard both imaging and sounding systems.

II. AMSU INSTRUMENT

The Advanced Microwave Sounding Units are flown onboard NOAA-15, -16, and -17 satellites. The instruments have been operational since 1998. The AMSU contain two modules: A and B. The A module (AMSU-A) has 15 channels (see Table I)

and is mainly designed to provide information on atmospheric temperature profiles, while the B module (AMSU-B) allows for profiling moisture structures. AMSU-A has an instantaneous field-of-view of 3.3° and scans $\pm 48.7^\circ$ from nadir with 15 different viewing angles at each side. The AMSU-A measures thermal radiation at microwave frequencies ranging from 23.8–9.0 GHz. Atmospheric temperature profiles are primarily based on the measurements obtained at channels near 60 GHz, which is an oxygen absorption band. In particular, the AMSU-A sounding channels (3–14) respond to the thermal radiation at various altitudes as shown by their weighting function distributions. Channels 1 and 2 detect clouds as well as surface properties [5]. Since the satellite provides a nominal spatial resolution of 48 km for AMSU-A at its nadir, the temperature perturbations from synoptic to mesoscale can be reasonably depicted. The AMSU-B instrument contains five channels (16–20; see Table I) and provides the atmospheric profile of moisture. The horizontal resolution of AMSU-B is 16 km at nadir. A combination of several AMSU imaging channels at frequencies of 31.4, 89, and 150 GHz has been utilized to determine cloud liquid and ice water contents, because they directly respond to the emission from liquid droplets and the scattering from ice particles [1]. AMSU channels are nonpolarized at nadir and mix-polarized off nadir. The polarization mixture reduces the angular dependence of the surface emissivity [2].

III. RETRIEVAL ALGORITHM

The 1D-var retrieval algorithm is composed of key components such as advanced radiative transfer models for computing radiances and gradient of radiance (or Jacobian), and a scheme for minimizing the cost function that weighs the relative contribution of background (*a priori*) information and satellite observations. The gradient of the computed radiance is with respect to the (background) state variables. Assuming that the errors in the observations and in the priori information are neither biased nor correlated, and have Gaussian distributions, the best estimate of \mathbf{x} will minimize the cost function

$$J = \frac{1}{2}(\mathbf{x} - \mathbf{x}^b)^T \mathbf{B}^{-1}(\mathbf{x} - \mathbf{x}^b) + \frac{1}{2}[\mathbf{H}(\mathbf{x}) - \mathbf{I}^0]^T \mathbf{R}^{-1}[\mathbf{H}(\mathbf{x}) - \mathbf{I}^0] \quad (1)$$

where \mathbf{B} is the error covariance matrix associated with the background state variable \mathbf{x}^b . \mathbf{R} is the sum of \mathbf{F} and \mathbf{E} . \mathbf{F} is the covariance error in the forward calculation and \mathbf{E} is the sensor noise, assuming that bias in measurements is calibrated out. The superscript T indicates a transpose. $\mathbf{H}(\mathbf{x})$ is the simulated radiance vector for a set of channels (or frequencies) at the state variable \mathbf{x} . \mathbf{I}^0 is the observed radiance vector. The error covariance matrices are often treated as diagonal matrices. In this study, we use the diagonal covariance matrix. Thus, the minimum of the cost function is found from an iterative process that computes a descent direction at the state \mathbf{x} . The value of the cost function gradient at each iteration is derived as

$$\nabla_{\mathbf{x}} J = \mathbf{B}^{-1}(\mathbf{x} - \mathbf{x}^b) + \mathbf{H}^T(\mathbf{x})\mathbf{R}^{-1}[\mathbf{H}(\mathbf{x}) - \mathbf{I}^0] \quad (2)$$

where \mathbf{H}^T is the adjoint operator of the Jacobian matrix. \mathbf{H} is the tangent linear function of H at point \mathbf{x} (where H here is the potentially nonlinear observation operator).

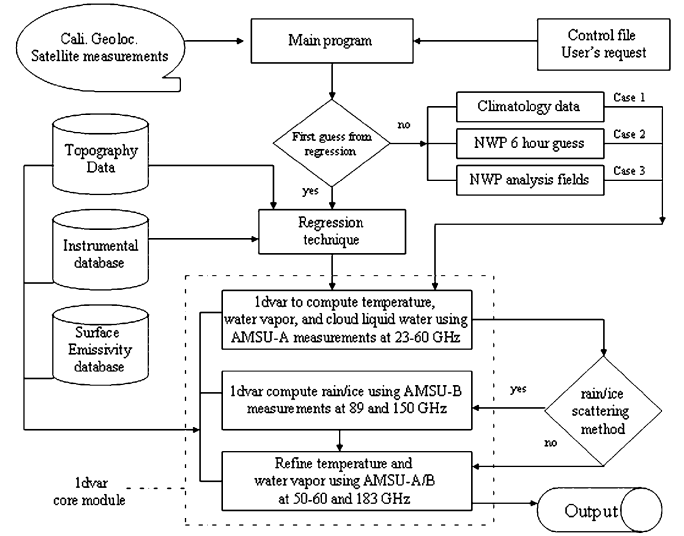


Fig. 1. Flowchart of the microwave 1-D variation algorithm. The core module describes the retrieval procedures.

An optimal solution to (2) is obtained by setting the gradient of the cost function zero and is expressed as follows [6]:

$$\mathbf{x}_{n+1} = \mathbf{x}^b + \mathbf{B}\mathbf{H}^T(\mathbf{x}_n)[\mathbf{H}(\mathbf{x}_n)\mathbf{B}\mathbf{H}^T(\mathbf{x}_n) + \mathbf{R}]^{-1}[\mathbf{I}^0 - \mathbf{I}(\mathbf{x}_n) - \mathbf{H}(\mathbf{x}_n)(\mathbf{x}^b - \mathbf{x}_n)] \quad (3)$$

if the number of unknowns is more than that of measurements. Alternatively

$$\mathbf{x}_{n+1} = \mathbf{x}^b + [\mathbf{H}^T(\mathbf{x}_n)\mathbf{R}^{-1}\mathbf{H}(\mathbf{x}_n) + \mathbf{B}^{-1}]^{-1} \times \mathbf{H}^T(\mathbf{x}_n)\mathbf{R}^{-1}[\mathbf{I}^0 - \mathbf{I}(\mathbf{x}_n) - \mathbf{H}(\mathbf{x}_n)(\mathbf{x}^b - \mathbf{x}_n)] \quad (4)$$

if the number of measurements is more than that of unknowns. In this study, (3) is applied due to the limited vertical resolution of AMSU data. Here the start point \mathbf{x}_1 is the first guess and the background \mathbf{x}^b represents the prior information.

Equations (3) and (4) can be iteratively calculated for a given set of initial values or for a first guess of unknowns. As shown in Fig. 1, the first guess can be obtained from several methods: numerical weather prediction model outputs, climatological databases, and regression algorithm outputs. An intelligent first guess can speed up the convergence to the final solution. In this study, a regression technique is used to get the first guess. The background for the atmospheric temperature and water vapor is taken from a forecast model. The background values for the cloud liquid water, rain water, and ice water profiles sets to zero or a small value. As shown in the core module within the dashed-dotted lines, the profiles of temperature, water vapor, and cloud liquid water are first calculated from AMSU-A channels 1–14. In this stage, the radiative transfer model is used for an initial assessment of these profiles. The AMSU-A measurements near 60 GHz are sensitive to the temperature profiles. The AMSU-A window channels are sensitive to total water vapor and cloud liquid water. The potential to derive the water vapor profile from AMSU-A measurements is determined by the sensitivity to total water vapor and the correlation between temperature and water vapor profiles. The second step is to retrieve rain water and ice water profiles associated with precipitation size particles using AMSU-B 89 and 150 GHz, assuming that the profiles of temperature, water vapor, and cloud liquid water are the same

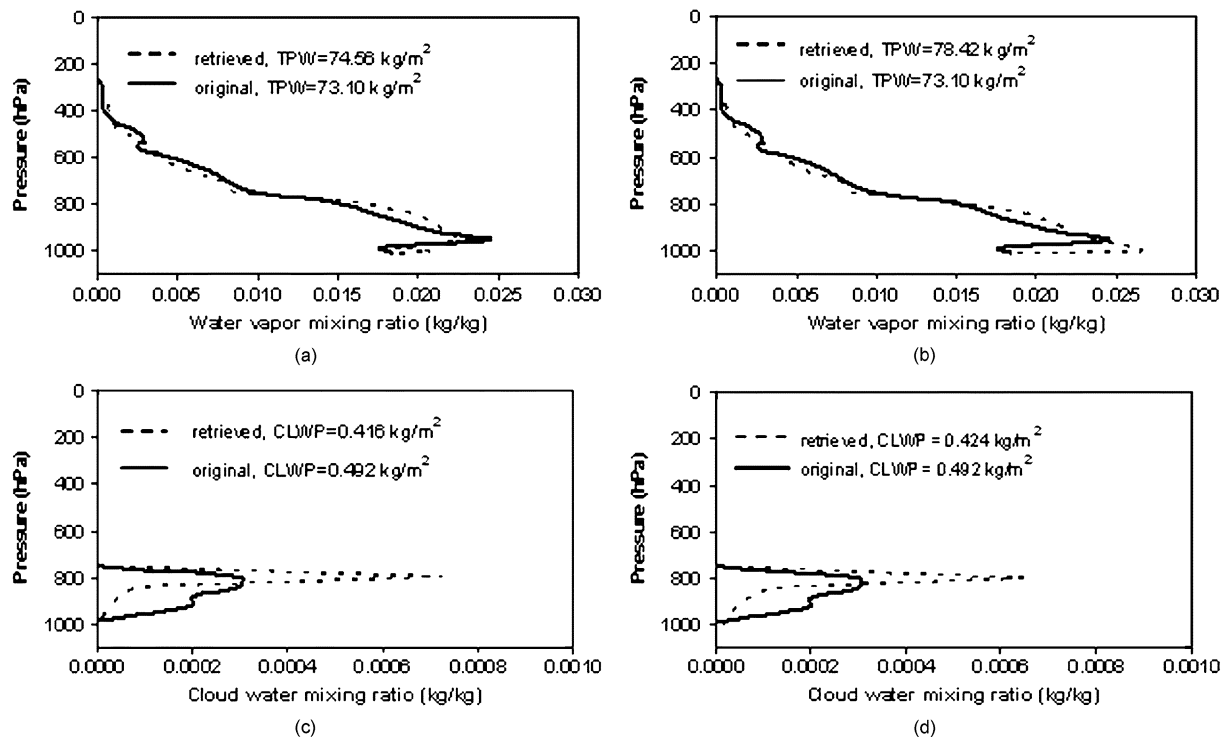


Fig. 2. (Top) Comparison of the original and retrieved water vapor profile over (a) ocean and (b) over land. (Bottom) Comparison of the original and retrieved cloud liquid water profile over (c) ocean and (d) over land. The profile is interpolated and extrapolated into 42 pressure levels from a radiosonde measured at 7° north, 151° east on July 2, 2002. This profile is placed on ocean and land, respectively.

as those from the first step. This assumption is physically sound because scattering signatures from the two channels are not strongly sensitive to the temperature and water vapor profiles [2]. The final step involves a refinement to the temperature and water profiles by using all AMSU-A/B channels at 50–60 GHz and 183 GHz. The 183-GHz water vapor measurements can improve the accuracy of the water vapor profile at middle and high altitudes. There is a small effect of the refinement on the calculations from the previous step, which would require an iterative scheme. By using the retrieved profiles from the third step as inputs to the second step, the identification of the rain and ice clouds remains the same. The retrieved rain water and ice water contents can be changed by about 2% for cloudy conditions. Due to the speed requirement in operational processing, only a flag is assigned to qualify the consistency. Note that at the second step, rain water, and ice water contents are calculated only when the scattering signatures at 89 and 150 GHz exceed a threshold [2].

The stability and convergence of the retrieval algorithm is a common issue. This retrieval algorithm takes three iterative cycles at each step to achieve the convergence, in general. The stability may be tested by perturbing the first guess (i.e., start point). For this algorithm, there is not a significant change between using the temperature and water vapor profiles as inputs from the regression method and from the retrieval at the last step.

An important process in Fig. 1 is to correct the various biases from the AMSU instrument, within the forward model and the first guess. It was found that three AMSU instruments on board NOAA-15, -16, and -17 satellites all display some level of asymmetric radiances across their scan line [1]. The causes for this asymmetry are still not fully understood. Nevertheless, an empirical algorithm was developed [1] and utilized in this

study. In addition to a correction of the instrumental bias, the biases of the first guess and forward model to the truth are also corrected. When using forecast model outputs (e.g., 6-h forecast) as a first guess, we collocate *in situ* temperature and water vapor profiles observed from radiosondes with forecast model outputs, and then calculate the global mean difference between the first guess and *in situ* data. The biases in the forward radiative transfer model are derived from the mean difference between measured brightness temperatures and simulated brightness temperatures that are calculated from radiosonde data.

The constant error covariance matrix \mathbf{B} associated with the background and the constant covariance error matrix \mathbf{R} associated with the observation error and the error in forward radiative transfer calculations are also important parameters in the 1D-var package [see (1) and (2)]. By definition, the background is the prior information and the first guess is the start point for solving a retrieval equation although the background can be used as the first guess. In (3) or (4), \mathbf{x}_1 is the first guess. After removing biases in the simulated brightness temperatures, the standard deviation of simulations to satellite observations is used for the error covariance matrix \mathbf{R} . A similar method is used to define the error covariance of the background. In this study, only diagonal elements of the background error covariance matrix are used. A detailed description of the observational and background error covariance is referred to <http://www.emc.ncep.noaa.gov/gmb/treadon/gsi/>.

In this study, the first guesses to temperature and water vapor profiles are derived from a regression algorithm [7], [8]. These guesses are obtained at a maximum of 42 levels from surface to 0.1 hPa in order to make this 1D-var generally applicable for the current satellite data assimilation system. It should be pointed out that an individual AMSU-A channel is not sensitive

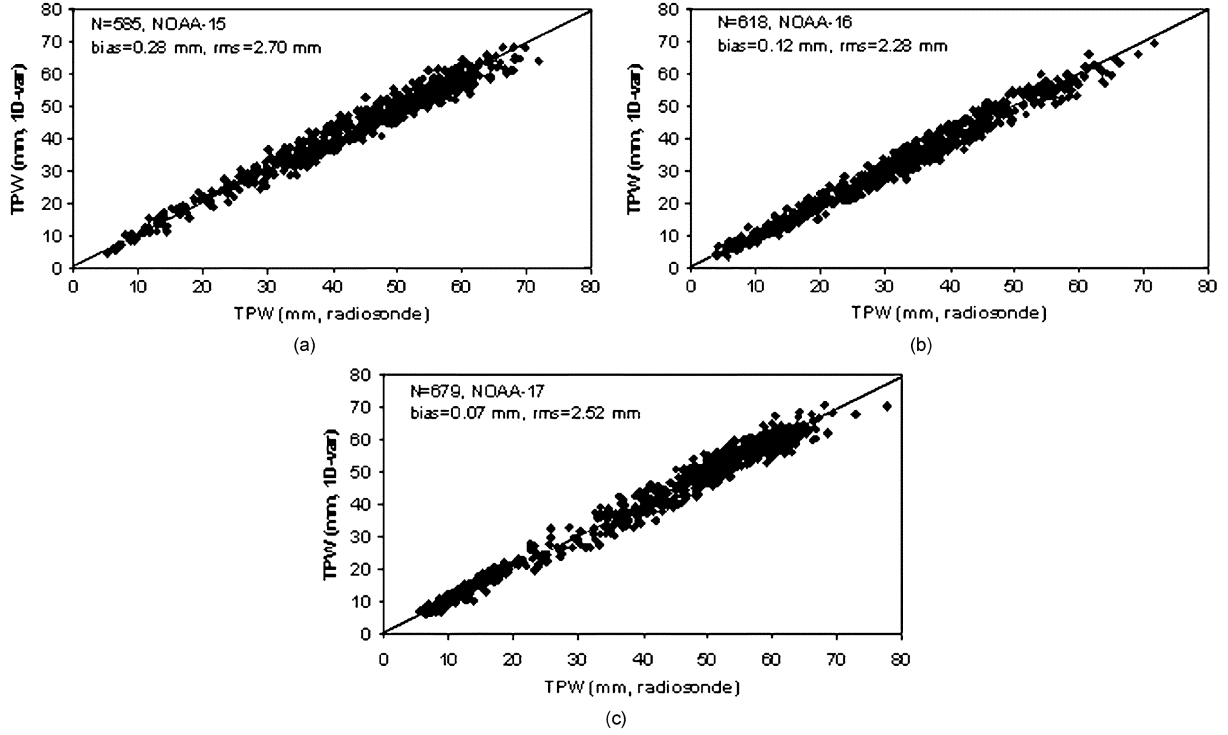


Fig. 3. Comparison of the total precipitable water between radiosondes and retrievals using data from (a) NOAA-15 AMSU, (b) NOAA-16 AMSU, and (c) NOAA-17 AMSU.

to water vapor profile. However, AMSU-A channels are sensitive to the total precipitable water vapor (e.g., 23.8 GHz) and vertical temperature profile. Thus, the initial water vapor profile can be still estimated from the AMSU-A because of the correlation between temperature and water vapor profiles, and the AMSU-A channel 1 sensitivity to the total precipitable water.

The regression coefficients for temperature and water vapor profiles are predetermined using our collocated radiosondes and satellite measurements. Note that the first guess for cloud water profile is set to zero above the freezing level and to a small value of $0.005 \text{ g} \cdot \text{m}^{-3}$ for the rest part of the profile, since the *in situ* cloud liquid water profile [9] is not sufficient for developments of the regression algorithm. Since the 1D-var procedure also retrieves the rain water profile, we need to identify the precipitating atmospheres. In doing so, the rain is determined through an algorithm which uses AMSU-B measurements at 89 and 150 GHz [2]. While the rain pixel is identified, a vertically uniform distribution of rain water below the freezing level is assumed.

The first guess of ice water content is assumed to be uniformly distributed above the freezing level if the scattering signature is larger than the threshold defined in [1]. The ice particle effective diameter is calculated from the scattering parameter ratio at 89 and 150 GHz, which in turn is defined as the ratio of the difference between predicted and measured brightness temperatures to the measured brightness temperature. The predicted brightness temperature is computed from AMSU-A channels 1 and 2 brightness temperatures based on a regression technique. The ice water path is then calculated from the effective diameter and the scattering parameter. Detailed information is to be found at <http://www.orbit.nesdis.noaa.gov/corp/scsb/mspps/main.html>.

As required by 1D-var, the surface pressure and ocean wind speed are taken from 6-h forecast data from the National Centers for Environmental Prediction (NCEP) global forecast system (GFS). A high-resolution dataset having a $1/6^\circ$ is used to define surface elevation and 24 surface types. The surface types are: water, old snow, fresh snow, compacted soil, tilled soil, sand, rock, irrigated low vegetation, meadow grass, scrub, broadleaf forest, pine forest, tundra, grass soil, broadleaf pine forest, grass scrub, oil grass, urban concrete, pine brush, broadleaf brush, wet soil, scrub soil, broadleaf 70-pine 30, and new ice.

IV. RADIATIVE TRANSFER MODEL

The radiative transfer model used in (1)–(4) is an improved version of the two-stream model [10]. In this model, the radiance emanating to the top of the atmosphere is first calculated at a fixed viewing angle using the two-stream solution. This radiance is then used to approximate the multiple scattering term in (5) as follows [11]:

$$-\mu \frac{dI(\tau, \mu)}{d\tau} = I(\tau, \mu) - \frac{\varpi}{2} \int_{-1}^1 P(\mu, \mu') \cdot I(\tau, \mu') d\mu' - (1 - \varpi)B(T) \quad (5)$$

where I is the intensity or radiance; ϖ the single-scattering albedo; $B(T)$ the Planck function of a temperature T , P the azimuth-averaged phase function. τ is the cumulative optical thickness increasing from 0 at the top of the atmosphere to τ_s at the surface.

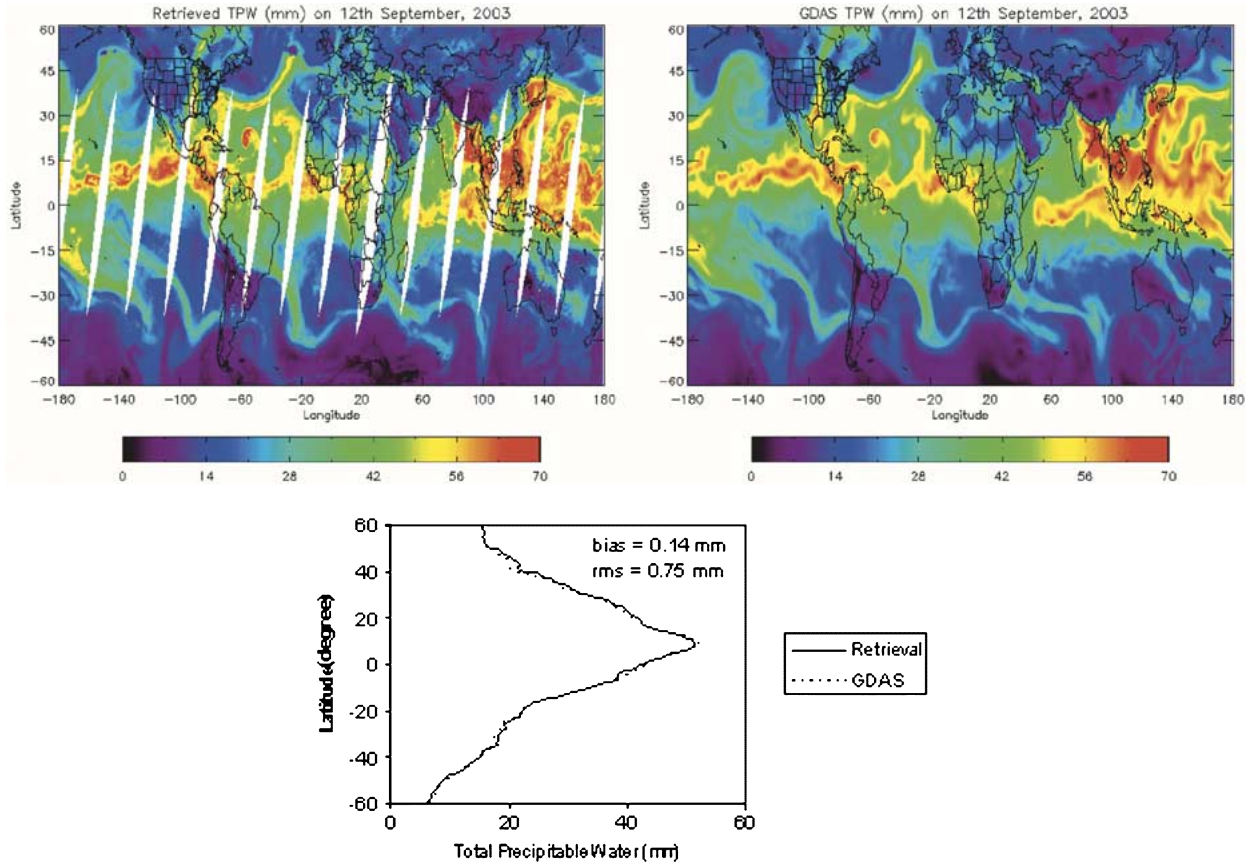


Fig. 4. Global distribution of the total precipitable water retrieved from (a) AMSU data, (b) from global distribution of the global data assimilation system (GDAS), and (c) the comparison of the zonal mean of total precipitable water between GDAS and retrievals.

The iterative solution to (5) can be derived accurately in terms of an integral form. For an optical depth of τ_b at a layer bottom, it can be written as

$$I(\tau, \mu) = I(\tau_b, \mu)e^{-\frac{\tau_b - \tau}{\mu}} + \int_{\tau}^{\tau_b} (1 - \varpi)B(T)e^{-\frac{\tau_b - \tau'}{\mu}} \frac{d\tau'}{\mu} + \int_{\tau}^{\tau_b} \int_{-1}^1 d\mu' \left[\frac{\varpi}{2} P(\tau', \mu, \mu') I(\tau, \mu') e^{-\frac{\tau_b - \tau'}{\mu}} \right] \frac{d\tau'}{\mu}. \quad (6)$$

The first term on the right side of (6) is the transmitted radiance from the bottom of the layer. The second term represents the emitted radiances by the layer which can be derived from the atmospheric temperature and optical parameters. The radiance from the first two terms on the right side is called path radiance, because they act in the same way as in the emission model. The path radiance approaches the exact emission solution when scattering approaches zero. The third term is the multiple scattering and can be evaluated using a two-stream solution. If more streams are used for multiple scattering, the solution as shown in (6) becomes more exact. However, in microwave frequencies, the two-stream solution [10] for the multiple scattering parts has resulted in a satisfactory accuracy of 1.0 K for simulated brightness temperature even under more cloudy conditions [10].

To speed up radiative transfer simulations, we use a fast model called OPTRAN [12], [13] to calculate atmospheric gaseous absorption at microwave frequencies. For a typical

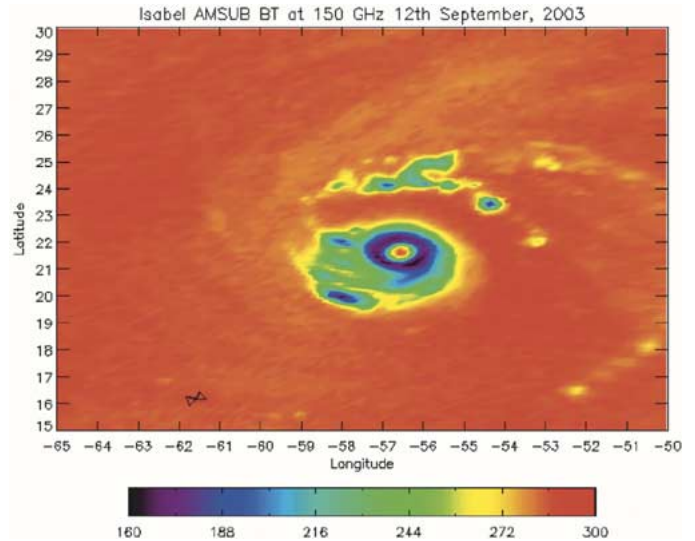


Fig. 5. Brightness temperatures at 150 GHz for a Hurricane Isabel scene on September 12, 2003.

AMSU channel with a finite frequency bandwidth, OPTRAN runs about 13 times faster than the typical microwave absorption model [14] calculation at a center frequency, and 100 times faster than the line-by-line calculations, where each band is cut with 10 lines. Furthermore, in comparison with the line-by-line calculations, OPTRAN can also achieve accuracy better than 0.1 K for all AMSU channels. Note that cloud optical properties

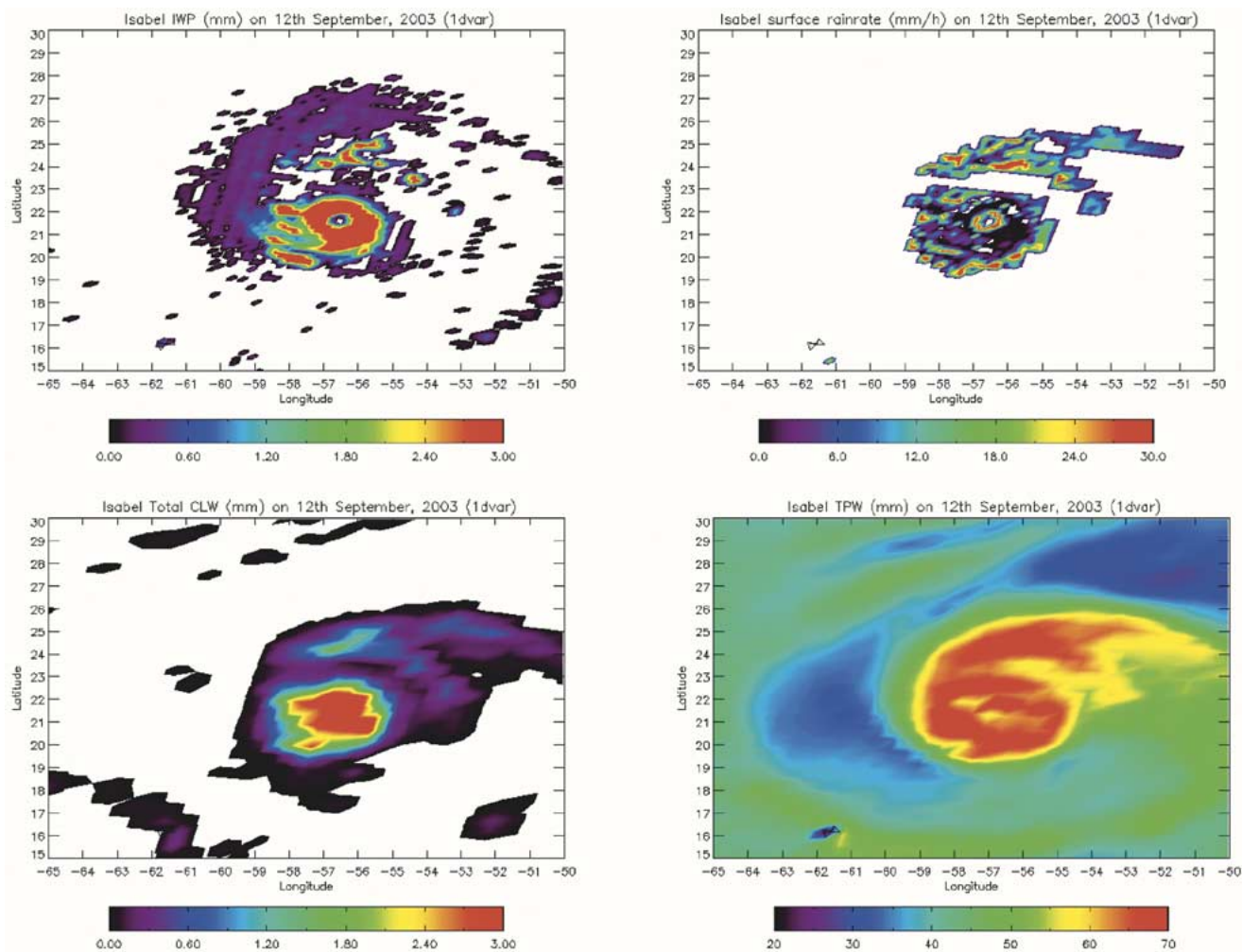


Fig. 6. (Top left) Retrieved ice water content, (top right) surface rain rate, (bottom left) cloud liquid water, and (bottom right) total precipitable water for Hurricane Isabel on September 12, 2003.

such as extinction coefficient, single albedo and asymmetry factor which are required in radiative transfer but not provided from OPTRAN are precalculated and made into a lookup table that can be used for faster retrievals.

As part of the radiative transfer model, various emissivity models are also needed to calculate the thermal emission from the earth's surfaces. For an oceanic surface, a fast emissivity model at microwave frequencies was developed and widely used for forward calculations [15], whereas for land, an emissivity model was also developed by Weng *et al.* [4] to compute the emissivity for a variety of surface conditions such as bare soil, canopy, and snow. These emissivity models are key components and are integrated in our 1D-var package.

V. RETRIEVAL RESULTS

The 1D-var retrieval algorithm is first tested using simulated AMSU brightness temperatures. In our simulations, atmospheric temperature and water vapor profiles from a radiosonde observation are interpolated and extrapolated into 42 pressure levels from 1050 hPa to 0.1 hPa. Five-layer clouds from 800–950 hPa are assigned to this radiosonde profile and the relative humidity from 800–950 hPa sets to 100%. Fig. 2(a)

and (b) displays water vapor profiles over oceans and land, respectively. In general, the retrieved water vapor profiles agree with original profiles. The water vapor derived in the profile peaks where clouds occur. The retrieval accuracy of total precipitable water over ocean [Fig. 2(a)] is better than over land [Fig. 2(b)], because microwave window channels measured over oceans are more sensitive to water vapor at lower altitudes in the troposphere. Fig. 2(c) and (d) shows the comparison of cloud liquid water over ocean and land, respectively. While the cloud liquid water paths agree, the vertical distributions are somewhat different. Retrieved cloud water concentrates near the cloud top due to a lack of detailed information on clouds from the AMSU sounding channels.

The 1D-var retrieval algorithm is also validated with collocated satellite measurements and radiosonde data. The radiosonde stations are distributed globally and are shown on the website <http://raob.fsl.noaa.gov/>. All AMSU and radiosondes data are matched with a spatial distance less than 50 km and a temporal difference less than 2 h. Fig. 3(a)–(c) compares the total precipitable water from radiosondes with that retrieved from NOAA -15, -16, and -17 AMSU data. Note that the entire match-up data during 2002 are used in this analysis and the comparisons are only made with the radiosonde data under

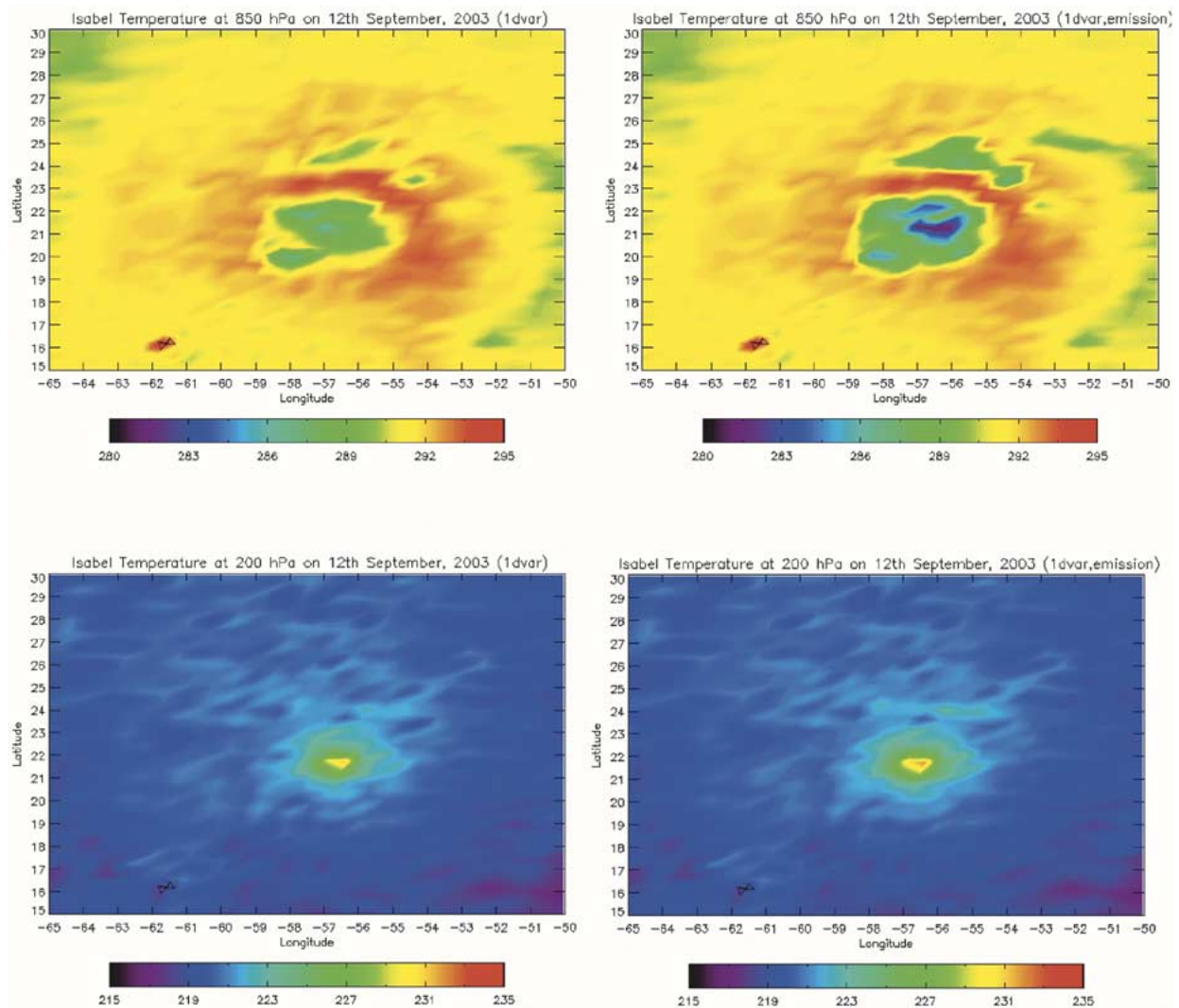


Fig. 7. Retrieved atmospheric temperature at 850 hPa through (top left) a scattering radiative transfer model and (top right) an emission radiative transfer model and (bottom left) the retrieved atmospheric temperature at 200 hPa through the scattering radiative transfer model and (bottom right) the emission radiative transfer model for Hurricane Isabel on September 12, 2003.

clear conditions. Overall, the biases are relatively small and root mean square error is stable and near 2.5 mm (or 2.5 kg/m^2), which is better than the results from our previous study [1].

The performance of the 1D-var algorithm is also tested using the global AMSU data over land and oceans but excluding the data over high latitudes beyond 60° north and south. Over land, surface parameters needed for emissivity calculations [4] are obtained from NCEP Global Forecast System (GFS), and include surface temperature, soil temperature, snow depth, vegetation coverage, canopy water content, land surface vegetation type, soil type, surface wind speed, and direction at 10 m above the surface, air temperature at 2-m height above the surface, and surface pressure. Fig. 4(a) and (b) compares the total precipitable water (TPW) derived from the AMSU and the GFS Data Assimilation System (GDAS). In general, AMSU retrieval agrees well with the GDAS data. Low TPW in the western United States, northern Africa, and southern Australia is obvious on both images. Hurricane Isabel having a higher amount of TPW locates at 21.75°N and 56.55°W . Fig. 4(c) further compares the zonal means of the TPW's between the

AMSU and GDAS data. The zonal mean is averaged over longitudes for clear and cloudy cases over land and oceans. Overall, the bias and rms error of the zonal means are 0.15 and 0.75 mm , respectively.

It is also important to assess the performance of the 1D-var under cloudy and precipitation conditions. In this study, the AMSU observations in Hurricane Isabel are used for our tests. Hurricane Isabel was one of the most powerful storms that affected the eastern portion of the United States in 2003. From the AMSU data at 150 GHz , we can clearly define the hurricane center near 21.75°N and 56.55°W and the spiral rainfall bands surrounding the eye (see Fig. 5). Fig. 6 shows retrieved cloud ice water path, surface rain rate, cloud liquid water path, and total precipitable water. Notice that the area covered by the cloud ice water is much broader than surface precipitation. The nonprecipitating ice clouds are primarily depicted by the AMSU 150 GHz . Also, both cloud liquid water and total precipitable water fail to detect the hurricane eye regions due to the poor spatial resolution of the AMSU data, although the amounts are generally higher near the center.

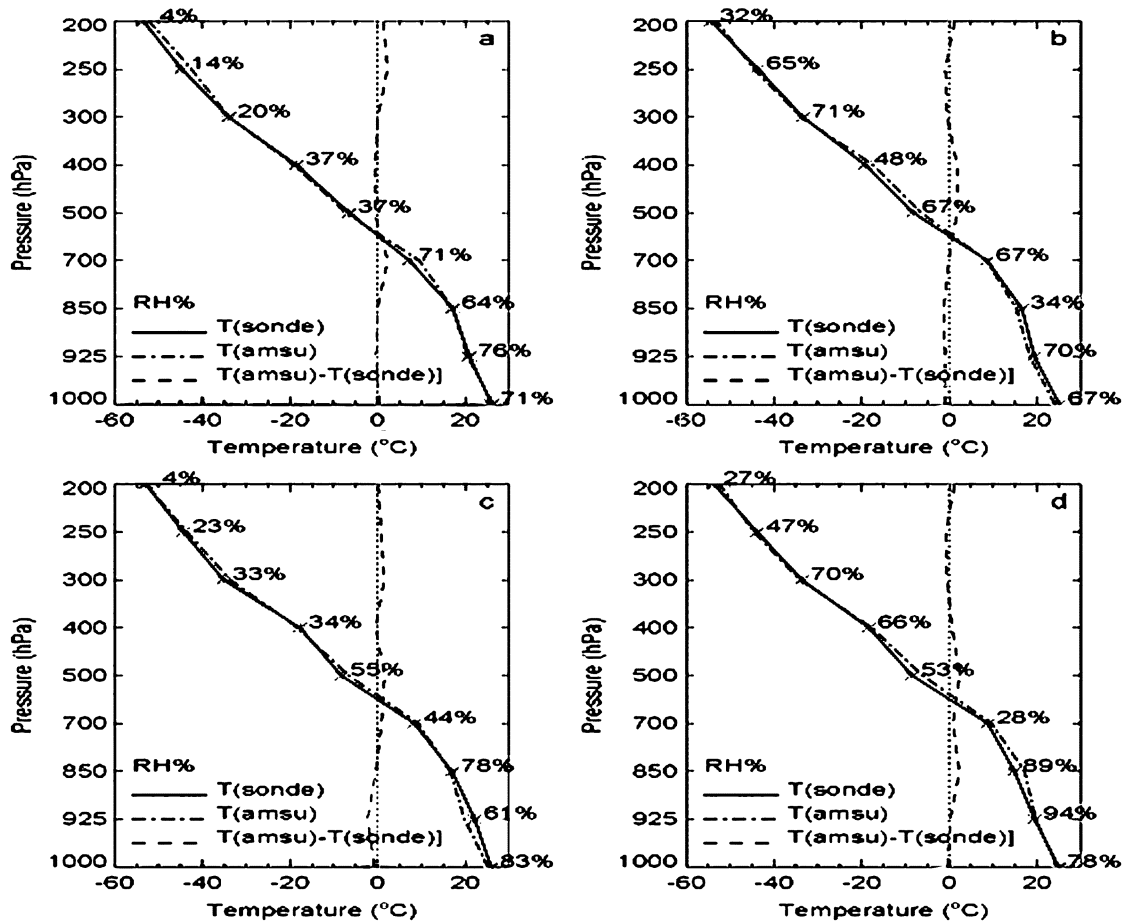


Fig. 8. Vertical distributions of the atmospheric temperatures from (solid line) dropsondes and (dashed-dotted line) the retrievals from AMSU measurements. The dashed lines are the difference of the atmospheric temperature between dropsondes and retrievals. The values in percentage represent measured relative humidity.

The effects of cloud and precipitation scattering on the temperature retrievals can be demonstrated by comparing the results from a scattering radiative transfer model to those from the emission-based model. In Fig. 7 (top left), the magnitude of the cold temperature anomaly at 850 hPa derived from the scattering model is more agreeable with other results [16], [17] than that from the emission-based in Fig. 7 (top right). Because of the scattering of liquid phase hydrometeors, the microwave brightness temperatures at sounding channels are strongly depressed. If this scattering effect would not properly taken into account in the retrieval process, the physical temperatures at 850 hPa would have been forced to the colder values which become highly nonphysical [see Fig. 7 (top right)]. Using the scattering model, the retrieved structure of cooling at 850 hPa is smooth, and the anomaly of about 3 K is realistic according to Hawkins and Rubsam [16].

The quality of the temperature distribution at 200 hPa has been also improved significantly using the scattering model. Note that the temperature at the center is about 10° warmer than that of its environment [see Fig. 7 (bottom left)] and is favorably comparable to other early observations [16], [17]. It is also interesting to see that the retrieved temperature from the emission model [Fig. 7 (bottom right)] is warmer than that from the scattering model [Fig. 7 (bottom left)], which is opposite to the pattern at 850 hPa. This can be explained as follows. For the

clouds at high altitudes, the transmittance in the emission model is smaller, attenuating the high radiance from lower warm and humid/cloudy atmosphere. Since the measured brightness temperatures are higher than those predicted by the emission-based model, the retrieval algorithm must enforce a warmer temperature there when the emission model is applied.

To validate the 1D-var retrievals, we also use collocated atmospheric temperature profiles from dropsondes and retrieved temperature profiles from AMSU for Hurricane Isabel. The comparison is carried out for Hurricane Isabel on September 16, 2003. Four dropsondes at $(-76.98^\circ, 31.20^\circ)$, $(-72.98^\circ, 33.61^\circ)$, $(-68.84^\circ, 33.55^\circ)$, and $(-67.01^\circ, 33.41^\circ)$ are matched with AMSU measurements at 06:00 UTC September 16, 2003. Fig. 8 shows the dropsonde measurements and retrievals at four sites. The differences between satellite retrievals and dropsondes measurements are typically less than 2 K. Even under heavy precipitation conditions [Fig. 8(d)], the retrieval errors are similar to those from other nonprecipitation cases indicating the algorithm robustness.

VI. SUMMARY AND DISCUSSION

This study develops a 1-D variation method (1D-var) for the retrieval of atmospheric temperature, water vapor, and cloud water. The scattering effects from clouds and precipitations are taken into account. Using an emission-based radiative transfer

model, the retrieved temperatures tend to be colder at lower altitudes and warmer at high altitudes. With a full scattering radiative transfer model, the quality of the retrieved temperature profiles can be significantly improved, and the retrievals agree well with coincident dropsonde's measurements.

The procedures developed in the 1D-var process have been optimized after our many numerical experiments. It is found that with measurements from AMSU-A channels 1–14, temperature profile and cloud liquid water can be first estimated. The AMSU-B window channel measurements can be then used to define cloud ice and rain water contents [1]. In our retrieval, the rain water is uniformly distributed below the freezing level, and the cloud ice water is also uniform above the freezing level. This treatment to the ice and rain water may be oversimplified. Thus, it is necessary to further refine all atmospheric parameters through an additional 1D-var process with all AMSU water vapor sounding channels near 183 GHz so that the water vapor products can be finally improved as well.

We use the same observational error and background error information throughout all steps in the retrieval. In the third step, the background information on the temperature and water vapor is the same as those from the first step. A refinement of temperature and water vapor profiles is necessary when rain or ice water is present, and when the measurements at 183 GHz become available for water vapor retrievals. Even without using the additional observations in the third step, the presence of rain, ice, or both modifies the sensitivity and the simulations, resulting in the modification of temperature and water vapor profiles.

There are numerous factors affecting the retrieval accuracy in atmospheric sounding [18]. For example, the different channels of satellite measurements are generally correlated, reducing the number of independent measurements on atmospheric structures. With fewer independent measurements, the detailed profiling of atmospheric structures becomes difficult. The magnitude of instrument noises also limits the retrieval accuracy. Furthermore, the systematic instrumental biases remaining after applying the empirical scan asymmetry correction may result in retrieval biases. A first guess that deviates less from the true profile can speed up the convergence and improve the retrieval accuracy.

ACKNOWLEDGMENT

The authors thank T. Zhu very much for his provision of Fig. 8. The authors express sincere thanks to the reviewers for their very helpful comments and valuable suggestions.

REFERENCES

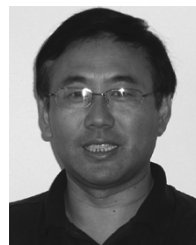
- [1] F. Weng, L. Zhao, R. Ferraro, G. Poe, X. Li, and N. Grody, "Advanced microwave sounding unit cloud and precipitation algorithms," *Radio Sci.*, vol. 38, pp. 8086–8096, 2003.
- [2] R. R. Ferraro, F. Weng, N. C. Grody, L. Zhao, M. Huan, C. Kongoli, P. Pellegrino, S. Qiu, and C. Dean, "NOAA operational hydrological products derived from the Advanced Microwave Sounding Unit (AMSU)," *IEEE Trans. Geosci. Remote Sensing*, vol. 43, no. 5, May 2005.
- [3] P. Schlüssel and W. J. Emery, "Atmospheric water vapor over oceans from SSM/I measurements," *Int. J. Remote Sens.*, vol. 11, pp. 753–766, 1990.
- [4] F. Weng, B. Yan, and N. C. Grody, "A microwave land emissivity model," *J. Geophys. Res.*, vol. 106, pp. 20 115–20 123, 2001.

- [5] S. J. English, "Estimation of temperature and humidity profile information from microwave radiances over different surface types," *J. Appl. Meteorol.*, vol. 38, pp. 1526–1541, 1999.
- [6] C. D. Rodgers, "Retrieval of atmospheric temperature and composition from remote measurements of thermal radiation," *Rev. Geophys.*, vol. 14, pp. 609–624, 1976.
- [7] J. Li, W. Wolf, W. P. Menzel, W. Zhang, H.-L. Huang, and T. H. Achor, "Global soundings of the atmosphere from ATOVS measurements: The algorithm and validation," *J. Appl. Meteorol.*, vol. 39, pp. 1248–1268, 2000.
- [8] J. R. Wang and L. A. Chang, "Retrieval of water vapor profiles from microwave radiometric measurements near 90 and 183 GHz," *J. Appl. Meteorol.*, vol. 29, pp. 1005–1013, 1990.
- [9] S. Crewell, G. Haase, U. Löhner, H. Mebold, and C. Simmer, "A ground based multi-sensor system for the remote sensing of clouds," *Phys. Chem. Earth (B)*, vol. 24, pp. 207–211, 1999.
- [10] Q. Liu and F. Weng, "A microwave polarimetric two-stream radiative transfer model," *J. Atmos. Sci.*, vol. 59, pp. 2396–2402, 2002.
- [11] K. N. Liou, *An Introduction to Atmospheric Radiation*. New York: Academic, 1980.
- [12] L. McMillin, L. J. Crone, M. D. Goldberg, and T. J. Kleespies, "Atmospheric transmittance of an absorbing gas. 4. OPTRAN: A computationally fast and accurate transmittance model for absorbing gases with fixed and variable mixing ratios at variable viewing angles," *Appl. Opt.*, vol. 34, pp. 6269–6274, 1995.
- [13] T. J. Kleespies, P. van Delst, L. M. McMillin, and J. Derber, "Atmospheric transmittance of an absorbing gas. 6. OPTRAN status report and introduction to NESDIS/NCEP community radiative transfer model," *Appl. Opt.*, vol. 43, pp. 3103–3109, 2004.
- [14] P. W. Rosenkranz, "A rapid atmospheric transmittance algorithm for microwave sounding channels," *IEEE Trans. Geosci. Remote Sensing*, vol. 33, no. 5, pp. 1135–1140, Sep. 1995.
- [15] S. J. English, "A fast generic millimeter-wave ocean emissivity model," in *Tech. Proc. 10th Int. TOVS Study Conf.*, J. Le Marshall and J. D. Jasper, Eds., 1999, pp. 178–183.
- [16] H. F. Hawkins and D. T. Rubsam, "Hurricane Hilda, 1964. II. Structure and budgets of the hurricane on October 1, 1964," *Mon. Weather Rev.*, vol. 96, pp. 617–636, 1968.
- [17] T. Zhu, D. Zhang, and F. Weng, "Impact of the advanced microwave sounding unit measurements on hurricane prediction," *Mon. Weather Rev.*, vol. 130, pp. 2416–2432, 2002.
- [18] C. D. Rodgers, *Inverse Methods for Atmospheric Sounding: Theory and Practice*. Singapore: World Scientific, 2000.



Quanhua Liu received the B.S. degree from the Nanjing Institute of Meteorology, Nanjing, China, the Master degree in physics from the Chinese Academy of Science, Beijing, and the Ph.D. degree in marine science from the University of Kiel, Kiel, Germany, in 1981, 1984, and 1991, respectively.

His primary interests are in radiative transfer theory, retrieval methodology, and applications of satellite data.



Fuzhong Weng received the Master degree in radar meteorology from the Nanjing Institute of Meteorology, Nanjing, China, and the Ph.D. degree from Colorado State University, Fort Collins, in 1985 and 1992, respectively.

He is currently a Physical Scientist and the Chief of the Sensor Physics Branch, Office of Research and Applications, National Oceanic and Atmospheric Administration, National Environmental Satellite, Data, and Information Service, Camp Springs, MD. From 2002 to 2004, he was the Deputy Director of

the Joint Center for Satellite Data Assimilation. From 1985 to 1987, he was an Instructor, teaching undergraduates courses on radar meteorology and in 1987 came to the United States to pursue his advanced studies in atmospheric sciences. He is a member of the NPOESS Microwave Operational Algorithm Team (MOAT) and has been actively involved in the NPOESS program.